

Kinetics and Mechanism of the (–)-Sparteine-Mediated Deprotonation of (*E*)-*N*-Boc-*N*-(*p*-methoxyphenyl)-3-cyclohexylallylamine

Daniel J. Pippel, Gerald A. Weisenburger, Neil C. Faibish, and Peter Beak*

Contribution from the Department of Chemistry, University of Illinois at Urbana–Champaign, Urbana, Illinois 61801

Received June 2, 2000

Abstract: The (–)-sparteine-mediated asymmetric lithiation–substitution of (*E*)-*N*-Boc-*N*-(*p*-methoxyphenyl)-3-cyclohexylallylamine (*E*-**5**) to afford γ -substituted enantiomerically enriched products **6** is reported. The solution structure for the lithiated intermediate **8•1** in these reactions was determined by heteronuclear NMR to be a configurationally stable, α -lithio, η^1 -coordinated monomer. This intermediate is proposed to exist as two rotamers that are rapidly equilibrating on the NMR time scale; competitive electrophilic substitution of each conformation results in the formation of *Z* or *E* products. Kinetic measurements of the lithiation by in situ infrared spectroscopy provide pseudo-first-order rate constants for reactions with a variety of concentrations of amine, (–)-sparteine, and *n*-BuLi. The reaction is first order in amine and zero order in 1:1 base–ligand complex. When the concentration of *n*-BuLi is varied independently of (–)-sparteine concentration, the reaction rate exhibits an inverse dependence on *n*-BuLi concentration. The deuterium isotope effect for the reaction was determined to be 86 at –75 °C, a result consistent with C–H bond breaking in the rate-determining step and indicative of tunneling. A reaction pathway involving a prelithiation complex is supported by kinetic simulations.

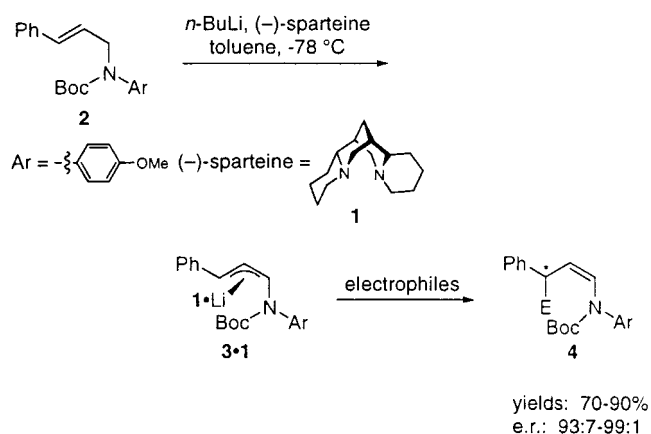
Introduction

Organolithium compounds are essential reactants or reagents in a majority of contemporary organic syntheses.^{1,2} Yet, reaction sequences that proceed via organolithium intermediates have been among the more difficult to characterize. Uncertainties related to aggregation states and the structures of the reactive species are problems that have to be resolved to unravel the course of most organolithium reactions.^{3–8}

In recent years, the applications of organolithium reagents have been extended by their applications to asymmetric syntheses. For these newly developed reactions, the stereochemical-determining steps must be delineated, and questions of absolute configuration, configurational stability, and stereochemical course of reaction become important.^{9–14} In this report, we provide an investigation into the kinetics and mechanism

of the asymmetric lithiation–substitution sequence of an *N*-Boc allylamine derivative for a (–)-sparteine-mediated deprotonation reaction.

Asymmetric lithiation–substitution sequences that provide homoenolate synthetic equivalents via dipole-stabilized carbanions have been reported for an oxygen-based system in seminal work by Hoppe, and for a nitrogen system from our laboratories.^{15–17} In our work, we have characterized the reaction pathways for the highly enantioselective (–)-sparteine (**1**)-mediated lithiation–substitution reactions of the cinnamylamine **2** to give enecarbamates **4**. The enantiodetermining step of



(1) Sapse, A.-M.; Schleyer, P. v. R. *Lithium Chemistry: A Theoretical and Experimental Overview*; John Wiley & Sons: New York, 1995.

(2) Wakefield, B. J. *The Chemistry of Organolithium Compounds*; Pergamon Press: New York, 1974.

(3) Recent leading work that focuses on the solution⁴ and solid-state⁵ characterizations of intermediates, determination of thermodynamic equilibria,⁶ the establishment of kinetic parameters for reactions,⁷ and the computational determination of structures and transition states⁸ is exemplary.

(4) Thompson, A.; Corley, E. G.; Huntington, M. F.; Grabowski, E. J. J.; Remenar, J. F.; Collum, D. B. *J. Am. Chem. Soc.* **1998**, *120*, 2028–2038.

(5) Hoppe, I.; Marsch, M.; Harms, K.; Boche, G.; Hoppe, D. *Angew. Chem., Int. Ed. Engl.* **1995**, *34*, 2158–2160.

(6) Streitwieser, A.; Wang, D. Z.-R. *J. Am. Chem. Soc.* **1999**, *1999*, 6213–6219.

(7) Sun, X.; Collum, D. B. *J. Am. Chem. Soc.* **2000**, *122*, 2452–2458.

(8) Würthwein, E.-U.; Behrens, K.; Hoppe, D. *Chem. Eur. J.* **1999**, *5*, 3459–3463.

(9) Hoppe, D.; Hense, T. *Angew. Chem., Int. Ed. Engl.* **1997**, *36*, 2282–2316.

(10) Beak, P.; Basu, A.; Gallagher, D. J.; Park, Y. S.; Thayumanavan, S. *Acc. Chem. Res.* **1996**, *29*, 552–560.

(11) Zschage, O.; Schwark, J.-R.; Kramer, T.; Hoppe, D. *Tetrahedron* **1992**, *48*, 8377–8388.

asymmetric deprotonation, the stereochemical course of substitution reactions, and the solid-state and solution structures

(12) Pearson, W. H.; Lindbeck, A. C.; Kampf, J. W. *J. Am. Chem. Soc.* **1993**, *115*, 2622–2636.

(13) O'Brien, P.; Powell, H. R.; Raithby, P. R.; Warren, S. *J. Chem. Soc., Perkin Trans. 1* **1997**, 1031–1039.

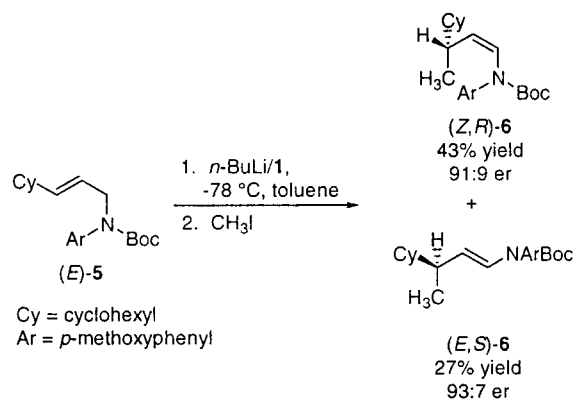
(14) Hoffmann, R. W.; Koverstein, R.; Harms, K. *J. Chem. Soc., Perkin Trans. 2* **1999**, 183–191.

of the lithiated intermediate have been reported.^{17–19} The sequence via **3·1** is of particular synthetic value as the employment of Michael acceptors as electrophiles provides 1,4-addition adducts with control over two newly generated stereogenic centers.^{20,21} Despite the well-developed synthetic, mechanistic, and structural aspects of this transformation, our efforts to obtain a complete kinetic profile and rate law for the metalation of **2** have been hampered by the high forward velocity of the reaction.²²

We now report that the lithiation–substitution of (*E*)-*N*-Boc-*N*-(*p*-methoxyphenyl)-3-cyclohexylallylamine ((*E*)-**5**) with *n*-BuLi/**1** (–)-sparteine (**1**) provides products with significant enantiomeric enrichments. For this reaction, we have established the enantiodetermining step and the diastereodetermining step, characterized the structure of the lithiated intermediate in solution, and determined the kinetics of the lithiation step.

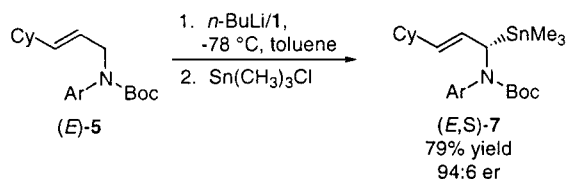
Results and Discussion

Deprotonation of (*E*)-**5** with *n*-BuLi/**1** at –78 °C in toluene followed by addition of 3 equiv of methyl iodide resulted in a 2:1 ratio of the γ -substituted products (*Z,R*)-**6** and (*E,S*)-**6**. The

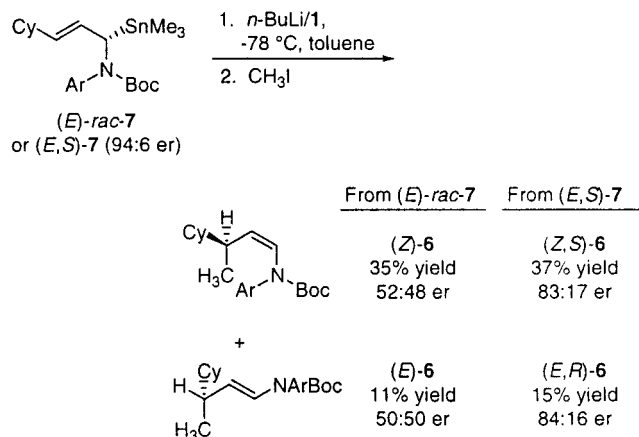


diastereomers are separable chromatographically, and the sequence thus provides access to either configuration at the γ -position. The absolute configurations of the products (*Z,R*)-**6** and (*E,S*)-**6** are assigned by analogy to those determined definitively for products arising from lithiation–substitution of (*E*)-**2**.¹⁷

The high γ -selectivity observed upon substitution with methyl iodide was not observed for the analogous reaction with trimethyltin chloride as the electrophile. In that case, the α -substituted product (*E,S*)-**7** was obtained in 79% yield with an enantiomeric ratio of 94:6.



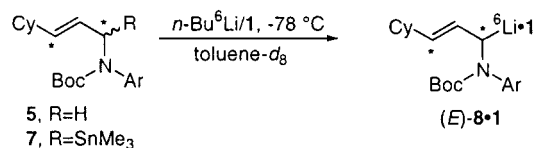
To determine whether the asymmetric induction for these reactions occurred in the substitution portion of the sequence, the racemic stannane (*E*)-*rac*-**7** was transmetalated with *n*-BuLi/**1**, and the resulting organolithium species was allowed to react with methyl iodide. This experiment provided the encarbamates (*Z*)-**6** and (*E*)-**6** in 46% overall yield with no enantiomeric



enrichment. The result shows that asymmetric substitution is not enantiodetermining and suggests that the enantiodetermining step in the formation of both the *Z* and *E* encarbamates from (*E*)-**5** is an asymmetric deprotonation that gives rise to configurationally stable intermediates.

The results from transmetalation–electrophilic substitution of enantiomerically enriched (*E,S*)-**7** also support the assignment of configurational stability to the intermediates in this sequence. In this case, the encarbamates **6** are formed in 52% overall yield with enantiomeric enrichment of 84:16. The configuration at the newly formed stereogenic center of both products is opposite to that obtained from the normal lithiation–substitution sequence. This result in conjunction with literature precedent suggests a stereochemical course for the reaction. Reactions of **8·1** with methyl iodide and trimethyltin chloride proceed antarafacially, while tin–lithium exchange occurs with retention of configuration.¹⁸

NMR Structure of the Lithiated Intermediate. Structure determination for the key intermediate(s) in this sequence was carried out and **8·1** obtained by lithiation of (*E*)-**5**, which was



¹³C-labeled at both allylic termini, with 0.9 equiv of *n*-Bu⁶Li/**1** in toluene-*d*₈ at –78 °C. The ⁶Li NMR and ¹³C NMR spectra of (*E*)-**8·1** are shown in Figure 1a and b.

The ⁶Li NMR has three signals centered at 1.17 ppm, consistent with two partially overlapping doublets in an 87:13 ratio with ¹*J*(⁶Li, ¹³C) = 4.2 Hz.²³ The spectrum is interpreted to indicate the presence of two monomeric η^1 complexes, (*E,R*)-**8·1** and (*E,S*)-**8·1**, in which each ⁶Li is bound to only one ¹³C atom. The absolute configurations for the major and minor

(21) Park, Y. S.; Weisenburger, G. A.; Beak, P. *J. Am. Chem. Soc.* **1997**, *119*, 10537–10538.

(22) The lithiation of (*E*)-**2** was demonstrated to be a very rapid process requiring less than 30 s. See Supporting Information section XIX for details.

(23) Two additional weak absorptions present at 0.71 and 0.72 ppm are unassigned.

(15) For a general review on chiral homoenolate synthetic equivalents, see: Ahlbrecht, H.; Beyer, U. *Synthesis* **1999**, 365–390.

(16) Behrens, K.; Fröhlich, R.; Meyer, O.; Hoppe, D. *Eur. J. Org. Chem.* **1998**, *1998*, 2397–2403.

(17) Weisenburger, G. A.; Faibish, N. C.; Pippel, D. J.; Beak, P. *J. Am. Chem. Soc.* **1999**, *121*, 9522–9530.

(18) Pippel, D. J.; Weisenburger, G. A.; Wilson, S. R.; Beak, P. *Angew. Chem., Int. Ed. Engl.* **1998**, *37*, 2522–2524.

(19) Weisenburger, G. A.; Beak, P. *J. Am. Chem. Soc.* **1996**, *118*, 12218–12219.

(20) Curtis, M. D.; Beak, P. *J. Org. Chem.* **1999**, *64*, 2996–2997.

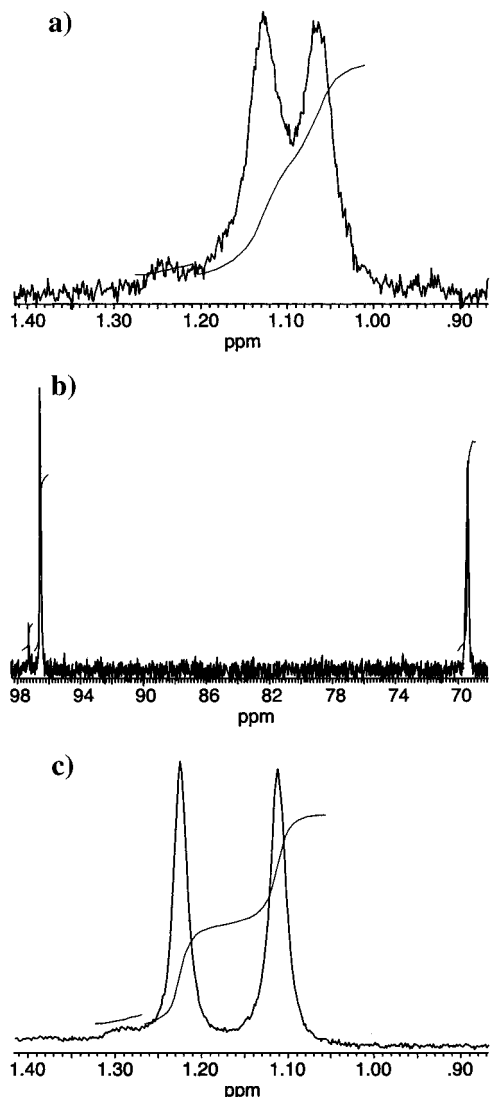


Figure 1. (a) 73.6-MHz ${}^6\text{Li}$ and (b) 125.7-MHz ${}^{13}\text{C}$ NMR spectra of (E,R) -**8•1** (${}^6\text{Li}$ and ${}^{13}\text{C}$ -labeled) in toluene- d_8 (0.10 M) at $-78\text{ }^\circ\text{C}$. (c) 73.6-MHz ${}^6\text{Li}$ spectrum of (E) -*rac*-**8•1** (${}^6\text{Li}$ labeled, no ${}^{13}\text{C}$ labels) in toluene (0.10 M) at $-78\text{ }^\circ\text{C}$.

diastereomers are based on analogy to the absolute configuration of **3•1**, which was determined through X-ray crystallography.¹⁸ In the corresponding ${}^{13}\text{C}$ NMR spectrum four total resonances are present, two at 97.3 and 96.5 ppm in a 15:85 ratio and two at 69.6 and 69.4 ppm in a 13:87 ratio. These signals are ascribed to the four allylic terminal carbons of (E,R) -**8•1** and (E,S) -**8•1**. The major absorptions at 96.5 and 69.4 ppm have a half-height line width of 10.6 and 16.3 Hz, respectively. The broadened signal at 69.4 ppm is ascribed to ${}^6\text{Li}$, ${}^{13}\text{C}$ coupling and is assigned to the carbon bearing the ${}^6\text{Li}$ atom.²⁴ On the basis of similar reasoning, the resonance at 69.6 ppm for the minor diastereomeric pair is assigned to the carbon bearing the ${}^6\text{Li}$ atom. Since the ${}^6\text{Li}$ NMR spectrum indicates that the organolithium species are monomeric, the ${}^{13}\text{C}$ absorptions at 69.6 and 69.4 ppm should be 1:1:1 triplets; however, the ${}^6\text{Li}$ - ${}^{13}\text{C}$ coupling was not resolved, presumably due to the greater natural line width.^{25,26}

To corroborate these assignments, an equimolar mixture of (E,R) -**8•1** and (E,S) -**8•1** was obtained from 1.0 equiv of *n*-

(24) To establish that the resonance at 69.4 ppm was properly assigned to the carbon α to nitrogen, a monolabeled variant of (E) -**5**, ${}^{13}\text{C}$ -labeled α to nitrogen, was prepared, deprotonated, and observed spectroscopically. See Supporting Information section V for details.

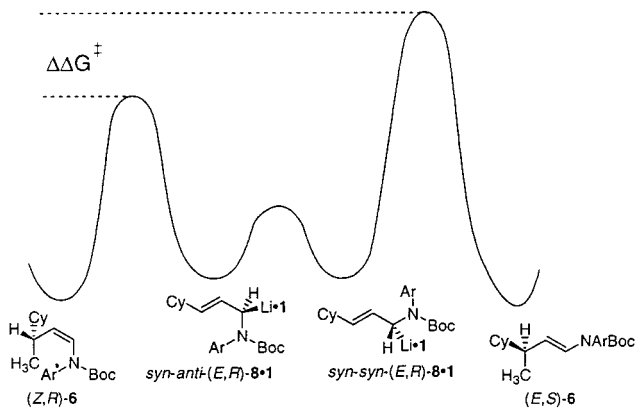
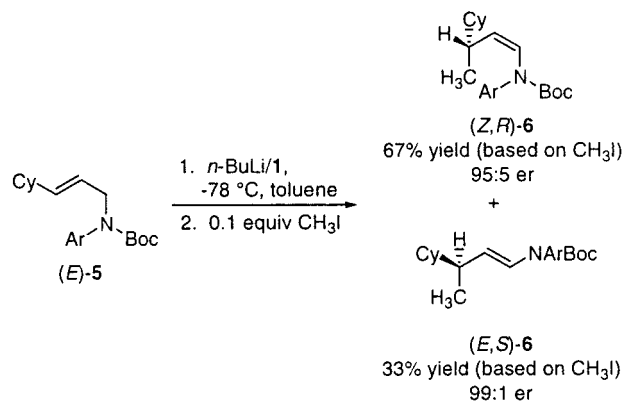


Figure 2. Reaction profile for dynamic, kinetically controlled reaction of *syn-anti*- (E,R) -**8•1** and *syn-syn*- (E,R) -**8•1** at $-78\text{ }^\circ\text{C}$.

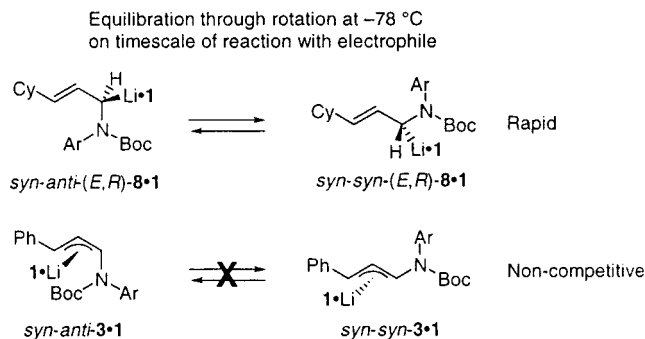
$\text{Bu}^6\text{Li}/1$ and the unlabeled α -stannane (E) -*rac*-**7**. The ${}^6\text{Li}$ NMR spectrum contains two singlets at 1.22 and 1.11 ppm in a 47:53 ratio as shown in Figure 1c.²⁷ Thus, the diastereomeric ratio (E,R) -**8•1** to (E,S) -**8•1** and ultimately the enantiomeric ratios of products **6** are not controlled by an equilibration process, but rather result from the mode of formation, consistent with the assignment of configurational stability to these species.

Origin of the Z/E Ratio. To explain the *Z/E* ratio in the reaction with methyl iodide, we hypothesize that the two rotamers *syn-anti*- (E,R) -**8•1** and *syn-syn*- (E,R) -**8•1** give rise to the diastereomeric products (Z,R) -**6** and (E,S) -**6**, respectively. Because only a single major diastereomeric intermediate is detectable in the NMR, *syn-anti*- (E,R) -**8•1** and *syn-syn*- (E,R) -**8•1** must rapidly equilibrate at $-78\text{ }^\circ\text{C}$ on the NMR time scale. To compare the rate of equilibration by rotation to the rate of reaction with electrophile, a modified version of Hoffmann's test for configurational stability was performed.^{10,28,29} Deprotonation of (E) -**5** with *n*- $\text{BuLi}/1$ at $-78\text{ }^\circ\text{C}$ in toluene followed



by addition of 0.10 equiv of methyl iodide resulted in a 2:1 *Z/E* product ratio. This ratio is identical to the result obtained with an excess of methyl iodide. These results are consistent with a dynamic, kinetically controlled process being the pathway that leads to the observed *Z/E* product ratio, as illustrated by the energy diagram shown in Figure 2.^{30,31}

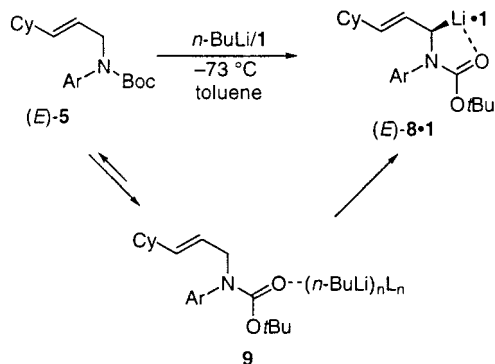
For reactions of the η^3 lithiated intermediate **3•1**, *Z/E* product ratios were typically found to be $>40:1$. The ratio was determined to be dependent on conversion, indicating that the intermediates leading to *Z* and *E* products were not rapidly equilibrating.¹⁷ It is not surprising that rotation about the C-1, C-2 bond of η^1 lithiated intermediate **8•1** is more facile than in the η^3 lithiated intermediate **3•1**.



Thus, the present work shows that at $-78\text{ }^{\circ}\text{C}$ (*E*)-**5** undergoes an asymmetric deprotonation to afford a kinetic ratio of the configurationally stable diastereomeric complexes (*E,R*)-**8•1** and (*E,S*)-**8•1**. Highly stereoselective electrophilic substitution provides the encarbamate product as a mixture of the *Z* and *E* isomers in a ratio that is established by a dynamic, kinetically controlled reaction of the rotamers *syn-anti*-(*E,R*)-**8•1** and *syn-syn*-(*E,R*)-**8•1**.

In Situ Infrared Spectroscopy. The course of the lithiation of (*E*)-**5** with *n*-BuLi/**1** can be followed by in situ infrared spectroscopy.^{7,32–35} The spectra for a sample reaction in which 1.2 equiv of *n*-BuLi was added to a premixed solution of 1 equiv of (*E*)-**5** and 1.2 equiv of (–)-sparteine in toluene at $-73\text{ }^{\circ}\text{C}$ are shown in Figure 3. The spectral baseline was reset to zero immediately prior to addition of *n*-BuLi, and 570 spectra were collected over a period of 600 s.

As shown in Figure 3, the absorbance associated with (*E*)-**5** at 1695 cm^{-1} rapidly decreases upon addition of *n*-BuLi as (*E*)-**5** is consumed. At a slower rate, an absorbance associated with **8•1** at 1640 cm^{-1} becomes increasingly positive.³⁶ A third absorbance at 1675 cm^{-1} is of particular interest. As shown in Figure 3a, this peak grows initially upon addition of base, but then slowly disappears as the reaction progresses. This absorbance is attributed to transient formation of a prelithiation complex, or complexes, **9**.^{37,38} Our long-standing interest in this



type of species prompted further investigation in attempt to determine whether the spectroscopically visible complex(es) **9** lie along the reaction pathway.³⁹

To determine reaction order in allylic amine, pseudo-first-order conditions were employed. High and constant concentra-

(25) In an attempt to increase the likelihood of observing coupling in the ^{13}C NMR spectrum, an additional experiment was performed using unlabeled *n*-BuLi/**1**. However, ^7Li , ^{13}C coupling was not resolved.

(26) The apparent presence of a single major intermediate on the NMR time scale is not inconsistent with the formation of the two products (*Z,R*)-**6** and (*E,S*)-**6** in a 2:1 ratio, as discussed in the next section.

(27) Additional weak absorptions at 0.60 and 1.29 ppm are unassigned.

(28) Hoffmann, R. W.; Rühl, T.; Harbach, J. *Liebigs Ann. Chem.* **1992**, 725–730.

(29) Hirsch, R.; Hoffmann, R. W. *Chem. Ber.* **1992**, 125, 975–982.

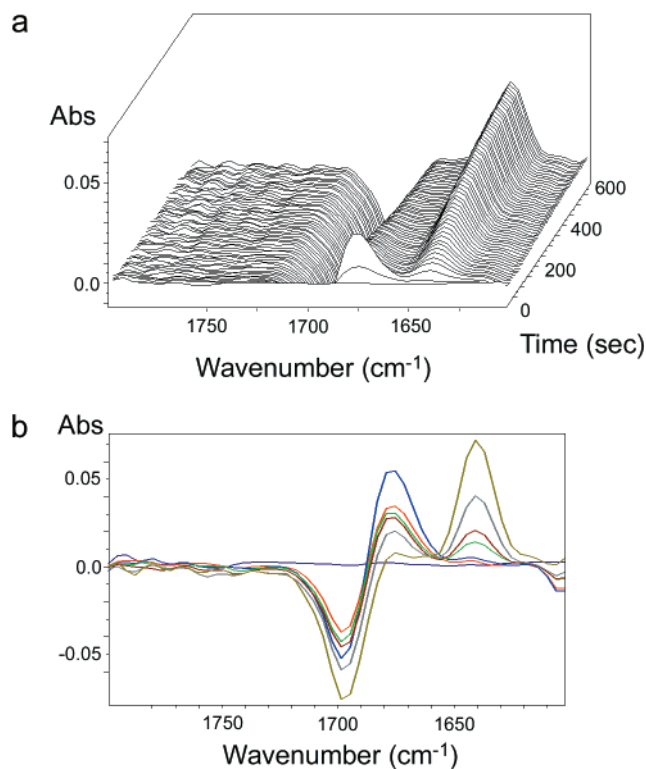


Figure 3. Progression of the (–)-sparteine-mediated stoichiometric reaction between (*E*)-**5** and *n*-BuLi in toluene as monitored by in situ infrared spectroscopy. (a) Three-dimensional plot of absorbance versus wavenumber versus time. (b) Several sequential two-dimensional infrared spectra taken at various times of the reaction.

tions of *n*-BuLi and **1** (0.66 M), were maintained for reactions executed over a 5-fold difference in initial allylic amine (*E*)-**5** concentrations (0.0236–0.005 06 M). For these reactions, (*E*)-**5**

(30) It is also conceivable that the rotamers do not equilibrate on the time scale of reaction with electrophile and that the activation energies for reactions with *syn-anti*-(*E,R*)-**8•1** and *syn-syn*-(*E,R*)-**8•1** are experimentally indistinguishable. In this case, the relative thermodynamic stabilities of the two rotamers would establish the ultimate *Z/E* ratio. Because the rotation is believed to be rapid on the NMR time scale and the reaction with electrophile is known to take in excess of 30 min, we assume that this possibility is unlikely.

(31) The ground-state energies of *syn-anti*-(*E,R*)-**8•1** and *syn-syn*-(*E,R*)-**8•1** are arbitrarily set as equal. Their relative values are, in fact, unknown.

(32) Al-Aseer, M.; Beak, P.; Hay, D.; Kempf, D. J.; Mills, S.; Smith, S. G. *J. Am. Chem. Soc.* **1983**, 105, 2080–2082.

(33) Hay, D. R.; Song, Z.; Smith, S. G.; Beak, P. *J. Am. Chem. Soc.* **1988**, 110, 8145–8153.

(34) Sun, X.; Kenkre, S. L.; Remenar, J. F.; Gilchrist, J. H.; Collum, D. B. *J. Am. Chem. Soc.* **1997**, 119, 4765–4766.

(35) All in situ infrared spectra were collected by means of an ASI ReactIR 1000 equipped with a 1.0-in. DiComp ATR probe (range 4400–2150, 1950–650 cm^{-1}). ASI Applied Systems, Inc., Millersville, MD 21108. See Supporting Information section I.E. for additional details.

(36) The lithiation of *N,N*-dimethyl-2,4,6-triisopropylbenzamide resulted in a shift from 1650 to 1588 cm^{-1} for the carbonyl stretching frequency.³⁵

(37) Contrary to expectation, the species responsible for the absorbance at 1675 cm^{-1} does not form instantly. Instead, after addition of base, the peak can be seen growing to maximum intensity over a period of several seconds. Because base–carbonyl complexation in the case of *N,N*-dimethyl-2,4,6-triisopropylbenzamide has previously been demonstrated by stopped-flow infrared spectroscopy to require less than 3 ms, we attribute the observation in our case to poor mixing.³³ For data that confirms the sluggishness of macromixing for the React-IR instrument as configured, see Supporting Information section XII.

(38) Addition of electrophile to the reaction mixture while the concentration of species **9** remained high resulted in the recovery of a significant amount of starting material. We interpret this result to indicate that **9** is, in fact, a prelithiation complex or complexes and not an isomer of a lithiated intermediate. See Supporting Information section XIV for details.

(39) Beak, P.; Meyers, A. I. *Acc. Chem. Res.* **1986**, 19, 356–363.

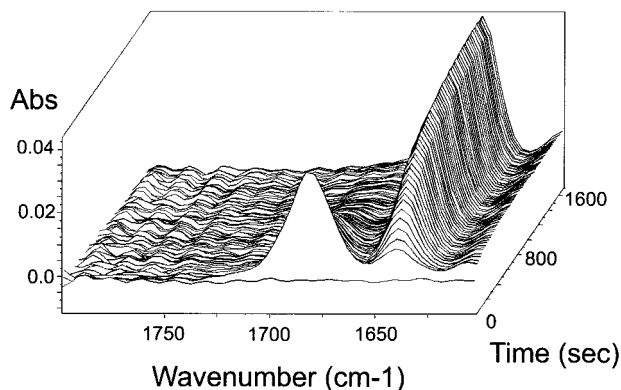


Figure 4. Three-dimensional infrared profile for the pseudo-first-order reaction between (*E*)-**5** and *n*-BuLi/1.

Table 1. Pseudo-First-Order Rate Constants and R^2 Values for Reactions Representing a 5-Fold Difference in Initial Carbamate Concentration

[<i>(E)</i> - 5] (M)	k_{obsd} (s^{-1})	R^2 (%)
0.0236	0.0021	99.1
0.0236	0.0022	99.2
0.0168	0.0023	99.1
0.00506	0.0021	98.2
0.00506	0.0019	97.4

was added last in a toluene solution. As shown in Figure 4 for the reaction of 1 equiv of (*E*)-**5** with 28 equiv of (–)-sparteine and *n*-BuLi at $-73\text{ }^\circ\text{C}$, a peak appeared at 1685 cm^{-1} upon addition of starting material.⁴⁰ This peak was gradually replaced by another peak at 1640 cm^{-1} , attributed to **8**·**1**. For each run, plots of $\ln(\text{abs})$ versus time proved linear and values for k_{obsd} remained constant, indicating that the reaction is first order in (*E*)-**5** with $k_{\text{obsd}} = 0.0021 \pm 0.0002\text{ s}^{-1}$ (Table 1).^{41,42}

To ensure that the product **8**·**1** acts as neither a catalyst nor an inhibitor of the reaction, a control experiment was performed. After completion of a pseudo-first-order reaction, the spectrometer was reset and a second aliquot of (*E*)-**5** was injected into the reaction mixture. Determination of pseudo-first-order rate constants for both reactions revealed values of k_{obsd} that were identical within experimental error.⁴³

In a control experiment aimed at verifying that the reactions observed under pseudo-first-order conditions are analogous to stoichiometric variants, 1 equiv of (*E*)-**5** was added to a solution of *n*-BuLi (13 equiv) and (–)-sparteine (13 equiv) in toluene at $-78\text{ }^\circ\text{C}$. After 30 min, 15 equiv of methyl iodide was added and the reaction was allowed to warm to room temperature. Relative to the normal sequence, yields of **6** were only slightly increased and enantiomeric ratios were only slightly eroded.

(40) In reactions where (*E*)-**5** is not present upon establishment of the spectral baseline, a broad peak at 1685 cm^{-1} appears upon its addition. The species contributing to this peak are most likely dependent upon the exact reaction conditions (vide infra).

(41) In a study aimed at ensuring that the React-IR response was linear over a range of absorbance values, the infinity absorbance points for the peaks at 1640 cm^{-1} were plotted versus expected concentration of **8**·**1**, assuming complete lithiation, for several reactions. The results show that the instrument response is linear; see Supporting Information section XIII for additional details. See also Supporting Information section XVIII for a discussion of errors in these measurements.

(42) At lower concentrations of (*E*)-**5**, the rate constant appears to still be valid, but poor signal-to-noise ratios preclude inclusion of these data. At higher initial concentrations of (*E*)-**5**, the rate constant increases in magnitude, and the process no longer appears to be first order in (*E*)-**5**. The cause of this phenomenon has not yet been determined.

(43) Both reactions exhibited clean first-order kinetics and rate constants were equivalent within 15%. See Supporting Information section XV for additional details.

Table 2. Pseudo-First-Order Rate Constants and R^2 Values for Reactions Representing a 39:1 to 19:1 Ratio of Base/Ligand Complex:Carbamate

base/ligand to (<i>E</i>)- 5	k_{obsd} (s^{-1})	R^2 (%)
39:1	0.0025	98.4
34:1	0.0030	98.8
29:1	0.0028	99.1
24:1	0.0027	97.5
19:1	0.0021	99.5

The results of this experiment imply that the reaction under pseudo-first-order conditions gives rise to the same intermediate, **8**·**1**, as the stoichiometric sequence.⁴⁴

To test for the dependence on the concentration of the base/ligand complex, a series of reactions in which the concentration of (*E*)-**5** was held constant at 0.017 M while the concentration of 1:1 *n*-BuLi/(–)-sparteine base/ligand complex was varied from 0.66 to 0.33 M were executed. From these reactions, it is apparent that the rate constant, k_{obsd} , changes neither significantly nor systematically as the ratio of base/ligand complex to (*E*)-**5** changes (Table 2). This apparent zero-order dependence on base/ligand complex is unprecedented and may be accounted for by the kinetic scheme shown in Figure 5.⁴⁵

In this scheme, a prelithiation complex, designated as **C**, is formed and the rate of product formation is directly proportional to the concentration of **C** (eq 1). This concentration may be expressed in terms of (*E*)-**5**, shown in Figure 5 as **A**, the concentration of base/ligand complex, **M**, and the equilibrium constant for the formation of **C** (eq 2).⁴⁶ Substituting the new expression for **C** into eq 1 results in eq 3. If it is assumed that the equilibrium represented by K_{eq} should significantly favor **C**, then the equation may be simplified such that the rate of product formation is dependent only on the rate constant $k_{\text{C} \rightarrow \text{P}}$ and the concentration of **A** (eq 4). Invoking a prelithiation complex seems appropriate in light of the spectroscopic observation of such a species.

Determination of Deuterium Isotope Effect and Arrhenius Parameters. To provide additional evidence for the mechanism and rate law proposed in Figure 5, k_{obsd} values were determined for several temperatures with both (*E*)-**5** and (*E*)-**5**- d_2 , which are isotopically substituted on the allylic carbon α to nitrogen. For these reactions, pseudo-first-order conditions were maintained with *n*-BuLi (0.36 M) and (–)-sparteine (0.33 M) present in 20-fold excess relative to (*E*)-**5** (0.016 M).⁴⁷ All reactions were performed in cumene as opposed to toluene, as cumene is less prone to decomposition at higher temperatures in the presence of high concentrations of *n*-BuLi and (–)-sparteine.⁴⁸ The data from these experiments are shown in Table 3 and an Eyring plot ($\ln k_{\text{obsd}}$ versus $1/\text{temperature}$) is shown in Figure 6.

(44) For complete details on these experiments, see section XIV of the Supporting Information.

(45) Gallagher, D. J.; Beak, P. *J. Org. Chem.* **1995**, *60*, 7092–7093.

(46) The *n*-BuLi/(–)-sparteine complex most likely exists predominantly as a dimer. However, the active metalating reagent is postulated for the purpose of the analysis in Figure 5 to be monomeric. The complete kinetic analysis in Figure 8 employs pseudospecies, as each of the components “base”, “base·(–)-sparteine”, and “complex” likely participate in multiple equilibria with higher order aggregates. The equilibrium constants in Figure 8, K_1 , K_2 , and K_3 , include the contributions from these equilibria.

(47) Reactions executed with an excess of *n*-BuLi relative to (–)-sparteine exhibit a decreased rate of reaction (vide infra). This was useful in retarding reactions of diprotio (*E*)-**5** at higher temperatures, which were too rapid for accurate determination of k_{obsd} with a 1:1 ratio of base to ligand.

(48) The substitution of cumene for toluene as the reaction solvent results in a slight increase in rate of reaction but provides the same products with similar diastereomeric and enantiomeric ratios. See Supporting Information section XIV for details.

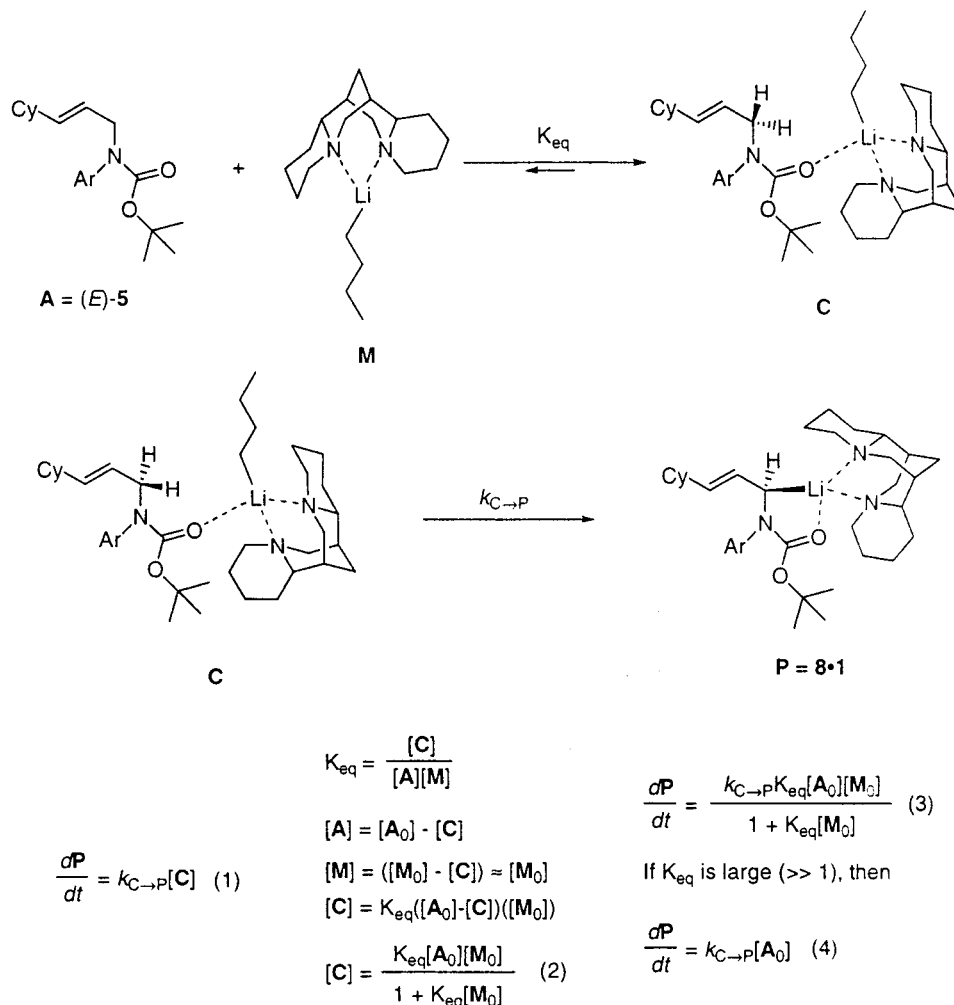


Figure 5. Proposed mechanism for lithiation of (*E*)-5 via a prelithiation complex.

Table 3. Variation in Pseudo-First-Order Rate Constant for Reactions of (*E*)-5 and (*E*)-5-*d*₂ at Several Temperatures

amine	temperature, °C	<i>k</i> _{obsd} (s ⁻¹)
(<i>E</i>)-5	-55	0.010 2
(<i>E</i>)-5	-65	0.005 10
(<i>E</i>)-5	-75	0.002 69
(<i>E</i>)-5- <i>d</i> ₂	-56	0.000 256
(<i>E</i>)-5- <i>d</i> ₂	-60	0.000 125
(<i>E</i>)-5- <i>d</i> ₂	-66.5	0.000 082 0
(<i>E</i>)-5- <i>d</i> ₂	-69.5	0.000 050 4
(<i>E</i>)-5- <i>d</i> ₂	-74	0.000 042 2
(<i>E</i>)-5- <i>d</i> ₂	-77	0.000 031 1

Thermodynamic parameters for lithiation of both (*E*)-5 and (*E*)-5-*d*₂ may be obtained from the plots in Figure 6 and are shown in Table 4. It should be emphasized that these values are rigorously accurate only if $k_{\text{C} \rightarrow \text{P}}$ may be closely approximated by k_{obsd} . This assumption is probably not entirely valid (vide infra). Nonetheless, we interpret the values for ΔS^\ddagger to be consistent with the transition state predicted by the mechanism in Figure 5.

From these reactions, we further conclude that there exists a high deuterium isotope effect that is consistent with C–H or C–D bond breaking in the rate-determining step for the reaction.⁴⁹ Both the magnitude of this deuterium isotope effect of 86 at -75 °C and 53 at -55 °C and the ratio of *A* values

(49) The observed effect is a combination of a primary isotope effect and a secondary isotope effect.

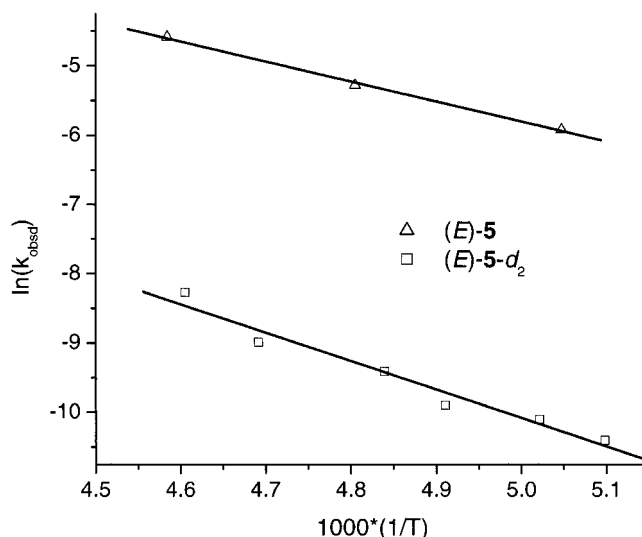


Figure 6. Eyring plot for deprotonation of (*E*)-5 and (*E*)-5-*d*₂.

($A_{\text{H}}/A_{\text{D}} = 0.39$) are consistent with the tunneling phenomenon.^{50–53}

(50) Kohen, A.; Klinman, J. P. *Chem. Biol.* **1999**, *6*, R191–R198.

(51) Melander, L.; Saunders: W. H. *Reaction Rates of Isotopic Molecules*; John Wiley & Sons: New York, 1980.

(52) Hoppe, D.; Paetow, M.; Hintze, F. *Angew. Chem., Int. Ed. Engl.* **1993**, *32*, 394–396.

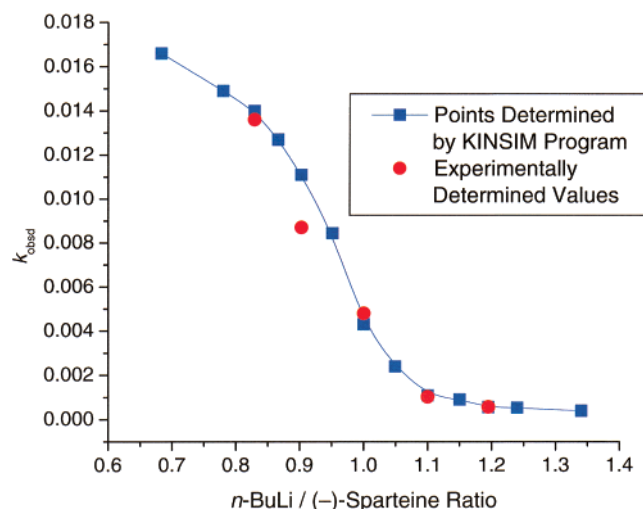
(53) Clayden, J.; Pink, J. H.; Westlund, N.; Wilson, F. X. *Tetrahedron Lett.* **1998**, *39*, 8377–8380.

Table 4. Thermodynamic Parameters for Deprotonation Reactions of (*E*)-**5** and (*E*)-**5-d**₂

thermodynamic parameter	303 K		200 K	
	(<i>E</i>)- 5	(<i>E</i>)- 5-d ₂	(<i>E</i>)- 5	(<i>E</i>)- 5-d ₂
E_a (kcal/mol)	6.03	8.24	6.03	8.24
A (s ⁻¹)	11,835	30,424	11,835	30,424
ΔH^\ddagger (kcal/mol)	5.43	7.64	5.63	7.84
ΔS^\ddagger (cal/mol)	-34.9	-33.0	-34.0	-32.2
ΔG^\ddagger (kcal/mol)	16.0	17.6	12.4	14.3

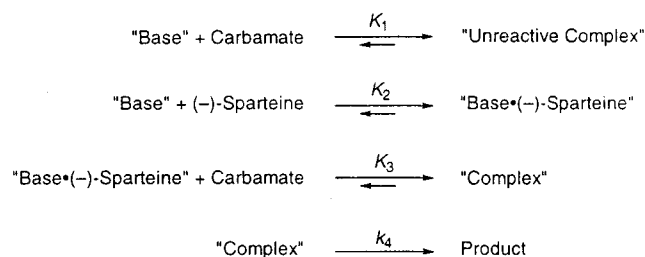
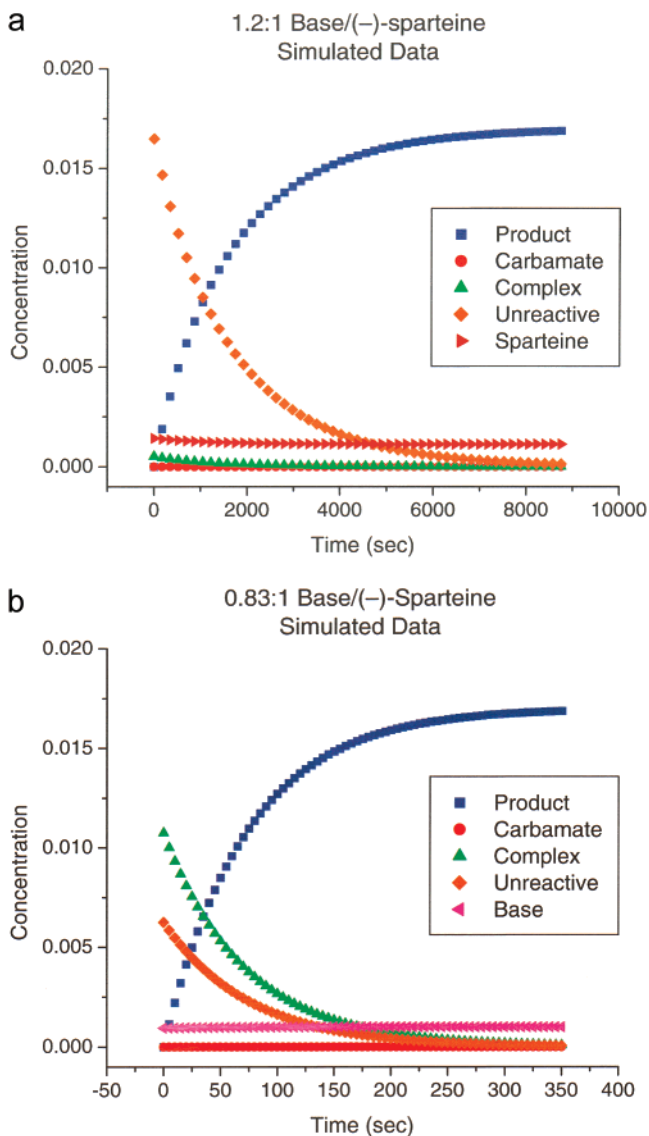
Table 5. Pseudo-First-Order Rate Constant for Reactions Employing Different Ratios of *n*-BuLi/(-)-Sparteine

<i>n</i> -BuLi/(-)-sparteine	k_{obsd} (s ⁻¹)	
	experimental	simulated
1.2	0.00057	0.00056
1.1	0.0010	0.0011
1.0	0.0048	0.0043
0.91	0.0087	0.011
0.83	0.014	0.014

**Figure 7.** Experimental and simulated data displaying inverse ratio between k_{obsd} and *n*-BuLi concentration at constant (-)-sparteine concentration.

Effects of Perturbing *n*-BuLi/(-)-Sparteine Ratio. The rate law derived in Figure 5 requires that the lithiation display a first-order dependence on (*E*)-**5**, but be independent of the concentration of any other species in the reaction mixture. This holds true as *n*-BuLi/(-)-sparteine concentrations are altered so long as the two reagents are maintained in a 1:1 ratio. However, if the concentration of *n*-BuLi is changed, while the concentration of (-)-sparteine is held constant, the rate of the reaction is impacted. This was demonstrated for the lithiation of (*E*)-**5** (0.017 M) by *n*-BuLi (0.34 to 0.49 M) in the presence of (-)-sparteine (0.41 M) in cumene (Table 5, Figure 7).

Surprisingly, the reaction rate constant shows an inverse dependence on *n*-BuLi concentration. As the concentration of *n*-BuLi increases from 0.34 to 0.49 M, the value of k_{obsd} decreases from 0.014 to 0.000 57 s⁻¹. One possible explanation for this effect considers an additional equilibrium in which excess *n*-BuLi may sequester the lithiation substrate (*E*)-**5** as a species designated as “unreactive complex” (Figure 8).⁴⁶ The facility of this mechanism to explain the experimental data was assessed through simulation and fitting routines performed using the software packages KINSIM and FITSIM.^{54–56} This exercise shows that the mechanism in Figure 8 adequately fits the experi-

**Figure 8.** Model for the lithiation of (*E*)-**5** which incorporates the inverse dependence on *n*-BuLi concentration.**Figure 9.** Simulated profiles for reactions with (a) excess and (b) deficient *n*-BuLi.

mental data if $K_1 = 1.3 \times 10^7$, $K_2 = 2.3 \times 10^4$, $K_3 = 2.6 \times 10^5$, and $k_4 = 2.19 \times 10^{-2}$. Simulated values for k_{obsd} at various *n*-BuLi/(-)-sparteine ratios are shown in Table 5 and Figure 7.

Additional insights into the mechanism may be gained through consideration of the reaction course for the most important species. Figure 9 shows the simulated reaction progress curves for product, carbamate, “complex”, “unreactive complex”, “base”, and (-)-sparteine at high (1.2:1) and low

(55) Barshop, B. A.; Wrenn, R. F.; Frieden, C. *Anal. Biochem.* **1983**, *130*, 134–145.(56) Zimmerle, C. T.; Frieden, C. *Biochem. J.* **1989**, *258*, 381–387.(54) <http://www.biochem.wustl.edu/cflab/message.html>.

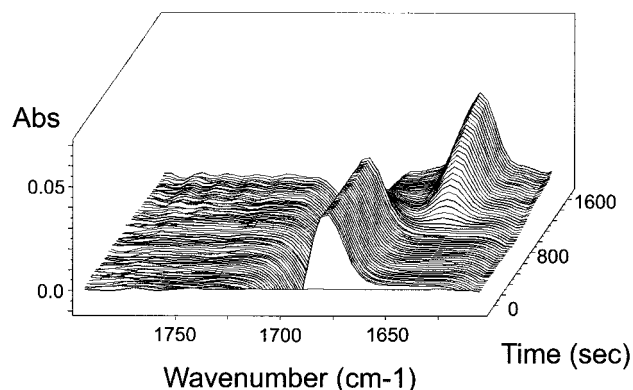


Figure 10. Three-dimensional profile showing the progression of reaction upon addition of *n*-BuLi at 10 s and addition of (–)-sparteine at 800 s.

(0.83:1) concentrations of *n*-BuLi relative to (–)-sparteine. It is apparent that under this model, at *n*-BuLi/(–)-sparteine 1.2:1, the dominant substrate species in the reaction mixture is the “unreactive complex”. The model also predicts that the concentration of free (–)-sparteine stays fairly constant throughout the reaction at ~ 0.002 M while the concentration of free “base” is off scale at ~ 0.075 M. In the case of deficient base, *n*-BuLi/(–)-sparteine 0.83:1, both “complex” and “unreactive complex” exist at similar concentrations with “complex” being present in slight excess. Here, “base” is present in a constant low concentration of ~ 0.001 M and (–)-sparteine is off scale at ~ 0.075 M. It is apparent that the higher the concentration of the “complex” at any given time, the greater the probability of productive forward reaction. The actual equilibria in solution are probably much more complex than those presented here with higher order aggregates also making significant contributions.⁴⁶ Nonetheless, this model is sufficient to explain the data in a semiquantitative manner that rationalizes the effect.

The dramatic acceleration of rate in the presence of excess (–)-sparteine relative to *n*-BuLi is of interest from a synthetic perspective. To gauge the generality of the phenomenon, the reactions were repeated with 1 equiv (*E*)-**5**, 1 equiv *n*-BuLi, and 1 or 2 equiv of (–)-sparteine.⁵⁷ In these cases, rate constants were determined using the method of initial rates. In fact, excess (–)-sparteine does increase the rate of reaction, even in reactions that are not under pseudo-first-order conditions; however, the magnitude of the effect is significantly smaller ($k_{\text{obsd}} = 0.0036$ s^{–1} with 1 equiv (–)-sparteine and $k_{\text{obsd}} = 0.0056$ s^{–1} with 2 equiv (–)-sparteine). Because this technique for increasing the rate of lithiation has synthetic potential, we determined the effect of 2 equiv of (–)-sparteine relative to *n*-BuLi on the reaction yield and selectivity. Metalation of **4** under these conditions and addition of methyl iodide gave rise to products **6** in normal yields and enantiomeric ratios: ((*Z,S*)-**6**, 44% yield, 91:9 er; (*E,S*)-**6**, 26% yield, 96:4 er).

(–)-Sparteine as a Reaction “Trigger”. The observed decrease in reactivity with decreasing concentration of (–)-sparteine relative to base suggested that the lithiation might not occur in the absence of ligand. A test of this hypothesis using the React-IR is shown in Figure 10. Addition of *n*-BuLi to (*E*)-**5** at time 10 s generates a stable carbamate-*n*-BuLi complex, as seen by the rapid appearance of a peak at 1675 cm^{–1}. Upon

addition of (–)-sparteine at time 800 s the deprotonation occurs, as evidenced by the slow increase in absorbance at 1640 cm^{–1}.⁵⁷ The potential for using this to develop a reaction that is catalytic in (–)-sparteine is recognized.⁵⁸ However, it would require an in situ electrophile that would react with the lithiated intermediate to release (–)-sparteine while remaining inert to free *n*-BuLi.

Conclusions

The work reported herein establishes that the structure for the lithiated intermediate in the lithiation–substitution reactions of (*E*)-**5** in solution is an α -lithio, η^1 -coordinated monomer. The results of the heteronuclear NMR study in conjunction with a Hoffmann-type test for configurational stability establish that the enantiomeric ratios of the products arise from an initial asymmetric deprotonation, while the *Z/E* ratio results from a dynamic, kinetically controlled reaction of rotamers in the substitution step. Pseudo-first-order rate constants were obtained for a variety of concentrations of amine, (–)-sparteine, and *n*-BuLi by monitoring the lithiation of (*E*)-**5** through in situ infrared spectroscopy. The reaction was found to be first order in (*E*)-**5** and display a zero-order dependence on 1:1 base/ligand complex, consistent with initial formation of a prelithiation complex. However, if the concentration of *n*-BuLi was varied independently of (–)-sparteine concentration, the reaction exhibited an inverse dependence on *n*-BuLi concentration. This behavior was simulated with a simplified reaction mechanism and optimized equilibrium and rate constants. If the model developed for the simulation is correct, then the spectroscopically observed prelithiation complexes **9** include both unreactive aggregates containing *n*-BuLi and carbamate and the reactive species formulated as (*E*)-**5**·*n*-BuLi·(–)-sparteine. The proposed model is supported by all experimental evidence including thermodynamic parameters, which were within expected ranges, and the observed high deuterium isotope effect. The establishment of a mechanism for the deprotonation of (*E*)-**5** is particularly valuable in that it serves as the best available model for the synthetically important lithiation of cinnamylamine (*E*)-**2**. This description of the lithiation of (*E*)-**5** by *n*-BuLi/(–)-sparteine in conjunction with our earlier analysis of deprotonation of (*E*)-**2** by the same base/ligand combination provides examples of asymmetric deprotonation leading to both localized and delocalized lithiated *N*-Boc allylic amines. The synthetic utility of these species is of continuing interest.

Acknowledgment. We thank both the National Institutes of Health (GM 18874) and the National Science Foundation (NSF-95-26355) for financial support of this work. D.J.P. acknowledges the DuPont Pharmaceutical Co. for an ACS Division of Organic Chemistry Graduate Fellowship. NMR experiments were performed in the Varian Oxford Instrument Center for Excellence NMR Laboratory (VOICE NMR Lab), in part funded by grants from the National Institutes of Health (PHS 1 S10 RR104-01), the National Science Foundation (NSF CHE 96-01502), and the Keck Foundation. We also gratefully acknowledge the assistance of Professors Stanley Smith, Alex Scheeline, and Wilfred van der Donk in data interpretation and the guidance of Professor David B. Collum and Jennifer L. Rutherford in successful application of the React-IR technology to our metalation reactions.

Supporting Information Available: General procedures for reactions, instrumentation, enantiomeric purity analyses, NMR

(57) In addition to considering the effects of excess (–)-sparteine and of no ligand, we also briefly explored the differences in reactivity for the TMEDA- and (–)-sparteine-promoted reactions. The (–)-sparteine reaction was found to be retarded relative to the TMEDA process by a factor of ~ 2 . See Supporting Information sections XVI and XVII for details.

(58) Carbolithiation reactions catalytic in (–)-sparteine have been reported: Norsikian, S.; Marek, I.; Klein, S.; Poisson, J. F.; Normant, J. F. *Chem. Eur. J.* **1999**, *5*, 2055–2068.

spectroscopic studies, and React-IR spectroscopic studies, as well as additional experimental details covering the syntheses of **5**, **6**, and **7**, syntheses of all isotopically labeled compounds, determination of mixing time for React-IR setup, determination of linearity of React-IR, data for lithiation in the presence of

TMEDA, control experiments, and application of React-IR monitoring to (*E*)-**2** (PDF). This material is available free of charge via the Internet at <http://pubs.acs.org>.

JA001955K